Environmental Chemistry Letters (2018) 16:389–400
https://doi.org/10.1007/s10311-017-0682-7

REVIEW

Nanoscale materials as sorbents for nitrate and phosphate removal from water

T. K. M. Prashantha Kumar[1] · Trivene R. Mandlimath[1,3] · P. Sangeetha[1] · S. K. Revathi[2] · S. K. Ashok Kumar[1]

Received: 22 November 2017 / Accepted: 23 November 2017 / Published online: 5 December 2017

Abstract

Excessive nitrogen (N) and phosphorous (P) release into run-off waters from human activities is a major cause of eutrophication. Several techniques are available to remove N and P-containing pollutants, such as chemical precipitation, biological treatment, membrane processes, electrolytic treatment, ion-exchange and adsorption. In order to remove low concentration levels of nitrate and phosphate, adsorption is a cost-effective solution. In this review, we present a list of nanoscale adsorbents such as zero-valent metal, metal oxides/metal hydroxides, and carbon-based materials. We discuss their adsorption capacities, isotherms, kinetics and mechanisms.

Keywords Eutrophication · Nanomaterials · Nitrate · Phosphate · Composite materials

Abbreviations

RO	Reverse osmosis
WHO	World health organization
USEPA	US environmental protection agency
EPA	Environmental protection agency
nZVI	Zero-valent iron
EDTA	Ethylenediamine tetracetic acid
MZVI	Micro-ZVI
La-ZFA	Lanthanum hydroxide-zeolite
C-cloth	Carbon cloth
OMM	Ordered mesoporous materials'
SBA	Santa Barbara amorphous
G-nZVI	Graphene-supported nanoscale zero-valent iron
CNT	Carbon nanotube
HZO	Nano-hydrous zirconium oxide
ppm	Parts per million
IEP	Isoelectric point

Introduction

Water played a crucial part in the origin of life, and it still has an essential role in maintaining plant and animal life. Plants depend on water for the transfer of nutrients and photosynthesis. The starting point of water pollution occurs when rain drops fall through the atmosphere they dissolve small quantities of gases in the atmosphere. Where there is little air pollution, the gases are mainly nitrogen, oxygen and a little carbon dioxide does make the water very slightly acidic owing to the production of weak carbonic acid. Rain falling in a thunderstorm is more acidic than normal. The energy of the lightning is sufficient to dissociate nitrogen molecules, which then combine with oxygen to give oxides such as nitrogen dioxide (Schumann and Huntrieser 2007). Once rain water contact with land surface, water pollution begins slowly depending upon distance travelled by water, and there may be following types of impurities present in the water (APHA 1985): dissolved impurities such as inorganic salt of the type MX, where M = Ca^{2+}, Mg^{2+}, Na^{+}, K^{+}, Fe^{2+}, Cu^{2+}, Al^{3+}; X = Cl^{-}, SO_4^{2-}, HCO_3^{-}, NO_3^{-}, PO_4^{3-}, F^{-} and NO_2^{-}; organic salts such as drugs and dyes; dissolved gases like O_2, CO_2, NO_x and SO_x and sometimes NH_3 and H_2S; toxic elements like Hg^{2+}, As^{5+}, Cr^{6+}, Pb^{2+}, Cd^{2+}; colloidal impurities like clay, silica, $Al(OH)_3$, $Fe(OH)_3$, humic acids; suspended impurities such as inorganic matters (clay and sand) while organic matters (oils globules, vegetables and animal matter); biological impurities such

✉ S. K. Ashok Kumar
ashok312002@gmail.com; ashokkumar.sk@vit.ac.in

[1] Department of Chemistry, School of Advanced Sciences, VIT University, Vellore, Tamil Nadu 632014, India

[2] Department of Chemistry, Nandi Institute of Technology and Management Sciences, Bangalore, Karnataka 560001, India

[3] Department of Chemistry, KPR Institute of Science and Technology, Arasur, Coimbatore, Tamil Nadu 641407, India

as bacteria and microorganism (virus, algae, fungi and diatoms). The standards for drinking water quality are typically set by governments or by international standards. These standards usually include minimum and maximum concentrations of contaminants, depending on the intended purpose of water use. Visual inspection cannot determine if water is of appropriate quality. Simple procedures such as boiling or the use of a household activated carbon filter are not sufficient for treating all the possible contaminants that may be present in water from an unknown source. This article is an abridged version of the chapter 8 published by Prashantha Kumar et al. (2016) describing the performance of various nanoscale materials for the removal of nitrate and phosphate ions.

Nitrate and phosphate pollution

The nitrate and phosphate substances are among the most problematic pollutants which significantly affecting the surface and groundwater all around the world. However, the nitrate and the phosphate pollution have been neglected by many countries. The rapid development of industrial and agricultural activities has taken over the human awareness on the effects of nutrients pollution to us and to the environment. Considering the bad effects of phosphate and nitrate pollution, WHO permits 5 ppm as the maximum level of phosphate, whereas for nitrate not more than 10 ppm is safe in drinking water (WHO 2011). A common cause of phosphate toxicity in humans includes impaired renal function, rhabdomyolysis and tumor lysis syndrome. In addition, exogenous phosphate toxicity is also documented in patients with Hirschsprung disease when exposed to hypertonic phosphate enemas (Razzaque 2011). When human consumes high concentration of nitrate through contaminated drinking water, there are high risks of being infected by diseases like methemoglobinemia, gastric cancer and non-Hodgkin's lymphoma (APHA 1998). Besides, the long-term exposure to nitrates and nitrites at level above maximum contamination level will cause diseases like diuresis, increased starchy deposits and hemorrhaging of the spleen (EPA 1990). Hence, the removal of nitrate and phosphate from wastewater prior to discharge is now necessary. Traditional methods for nitrates removal from waste water are biological denitrification processes, ion-exchange, reverse osmosis, electrodialysis and chemical denitrification. Among these methods, the first four methods have been applied in industry.

Biological denitrification process

In this process, nitrate is converted to nitrogen gas by denitrifying bacteria in the absence of oxygen ($NO_3 \rightarrow NO_2 \rightarrow NO \rightarrow N_2O \rightarrow N_2$). In order to satisfy the growth and energy requirements of the bacteria, methanol in excess of 25–35% must be added as a source of carbon. The removal efficiency ranges from 60 to 95%. The major advantage to anaerobic denitrification is that there are no waste products requiring disposal, produce a nontoxic by product (N_2), suitable for large applications, can handle high concentrations and destructive method. Some of the disadvantages of this method like electron donor and carbon source required, require downstream treatment (e.g., ozonation), high-maintenance, long start-up times, pH temperature sensitive and membrane fouling. Besides, there is no report for biological method for phosphate removal.

Ion-exchange process (IEP)

In the IEP, wastewater is passed through a media bed which removes both anionic phosphorus and anionic nitrogen ions and replaces them with another ion from the media. The exhausted resin will be regenerated using a concentrated solution of brine. Besides, this technique found to be stable, quick removal, easily automated, cost-effective, low maintenance and nondestructive. Difficulties in the process may be caused by fouling of the IE resin due to organic backbone and reduction in the exchange capacity due to sulfates and other ions.

Reverse osmosis (RO)

In this process, water begins to flow in the reverse direction with the application of pressure (750 psi) higher than the value of osmotic pressure. The pressure required to force the permeation through the membrane is dictated by the osmotic pressure of the feed stream. Membranes are generally made of materials such as cellulose acetate, polyamides and composite materials. The disadvantages associate with this process are due to membrane fouling, expensive energy, large capital costs and require treatment or disposal of concentrate. In addition, some nitrate and phosphate ions escape through the membrane (efficiency about 65–95%). Advantages of this technique are good for waters with high TDS content, no by-products and nondestructive.

Electrodialysis (ED)

ED is a nonselective demineralization process which removes all ions including nitrate and phosphate ions. ED

is accomplished by making cation and anion from aqueous solutions pass through IE selective membranes using the driving force of an electric field. When electric current is applied, the cations pass through the cation-exchanging membranes in one direction and the anions pass through the anion-exchanging membranes in the other direction (Hell et al. 1998). Disadvantages in the operation of this process include membrane clogging and precipitation of low-solubility salts of the membrane.

Chemical precipitation

Chemical precipitation is a flexible technology allowing for application of the metal salts at several stages during wastewater treatment (EPA 2000; Jiang and Graham 1998). Precipitation of phosphorus in wastewater may be accomplished by the addition of such coagulants as lime, alum, ferric salts and poly-electrolytes either in the primary or in the secondary state of treatment or as a separate operation in tertiary treatment. In general, large doses in the order of 200–400 ppm of coagulant are required. However, subsequent coagulation and sedimentation may reduce total phosphates to as low as 0.5 ppm, as in the case of lime. The removal of nitrate contents by this method not yet reported.

Adsorption method

Adsorption was first observed by C. W. Scheele in 1773 for gases, followed by Lowitz's experiments in 1785 for solution (Kraemer 1930). Adsorption is the accumulation of a substance at a surface or the interface between two phases. The adsorption process occurring at liquid–solid is a special interest from the water and wastewater treatment point of view. Adsorption takes place by physical forces or sometimes, chemical bondings also participate in adsorption process. A molecule adhered to the solid surface is called an adsorbate, and the solid surface as an adsorbent. When adsorption is concerned, thermodynamic and kinetic aspects should be involved to know more details about its performance and mechanisms. From the kinetic analysis, the solute uptakes rate, which determines the residence time required for the completion of adsorption reaction. Further, the solid–liquid adsorption process is influenced by parameters such as pH, solubility of solute in the solvent, solution temperature and also the initial solute concentration.

Adsorption isotherms and kinetics

Adsorption equilibrium is the set of conditions at which the number of molecules arriving on the surface of the adsorbent equals the number of molecules that are leaving. The relation between the amount of substance adsorbed by an adsorbent and equilibrium concentration of the substance at constant temperature is called the adsorption isotherm (Theodore and Ricci 2010). In order to determine the adsorption isotherm, several models have been suggested such as the Langmuir, Freundlich, Temkin, Elovich liquid film diffusion, intra-particle diffusion and Dubinin–Radushkevich isotherm models (Table 1). The applicability of the isotherm equation to the adsorption study done was compared by judging the correlation coefficients (R^2) (Tan et al. 2008). The study of adsorption kinetics is important because it provides valuable information and insights into the reaction pathways and the

Table 1 Isotherm constant parameters and correlation coefficients calculated for various adsorption onto various adsorbent

Phenomenon	Formula	Description of terms
Sorption studies	$q_t = \frac{V(C_0 - C_t)}{W}\ q_e = \frac{V(C_0 - C_e)}{W}$	C_t = adsorbate amount at time t C_0 = initial adsorbate amount V = volume of the solution W = weight of adsorbent
Langmuir isotherm	$\frac{C_e}{q_e} = \frac{C_e}{q\max} + \frac{1}{q\max K_L}$	C_e is the equilibrium concentration (mg/L) q_e is the amount of the phenol adsorbed at equilibrium (mg/g) $q_{\max}$ is the maximum adsorption capacity K_L is the Langmuir constant related to energy of the adsorption (L/mg) C_0 is the initial concentration of adsorbate in the liquid phase (mg/L)
Separation factor	$R_L = \frac{1}{1 + K_L C_0}$	If $R_L > 1$ unfavorable adsorption; $R_L = 1$ linear adsorption; $0 < R_L < 1$ favorable adsorption and $R_L = 0$ irreversible adsorption
Freundlich isotherm	$\ln q_e = \ln K_F + \frac{1}{n} \ln C_e$	K_F (L/mg) and $1/n$ are Freundlich constants giving an indicator of the adsorption capacity and the adsorption intensity
Temkin isotherm	$q_e = \frac{2.303RT}{b_T} \log a_T + \frac{2.303RT}{b_T} \log C_e$	b_T is the Temkin constant related to the heat of adsorption (J/mol) a_T is the Temkin isotherm constant (L/g), R is the gas constant (8.314 J/mol K), T is the absolute temperature (K)
Dubinin and Radushkevich (D–R)	$\ln q_e = \ln Q_s - B\varepsilon^2$	The slope of the plot of ln (q_e) versus ε^2 and the intercept yields the adsorption capacity, Q_s (mg/g). ε is Polanyi potential (kJ/mol)

Table 2 Key kinetic and thermodynamics parameters for the adsorption onto various adsorbent

Pseudo-first-order kinetic	$\log\left(q_e - q_t\right) = \log q_e - \frac{k_1}{2.303}t$	q_t is the amount of phenolic compounds adsorbed at time t (mg/g), k_1 is the first-order rate constant (min^{-1}) and t is a time in min log $(q_e - q_t)$ versus t to give a linear relationship from which k_1 and q_e can be determined from the slope and intercept
Pseudo-second-order kinetic	$\frac{t}{q_t} = \frac{1}{k_2 q_e^2} + \frac{t}{q_e}$	k_2 is the pseudo-second-order rate constant (L/mg min). (t/q_t) versus t to give a linear relationship from which $k1$ and q_e can be determined from the slope and intercept
Intra-particle diffusion model	$q_t = k_{id} t^{\frac{1}{2}} + C_i$	k_{id} is the intra-particle diffusion rate constant (mg/g/min1/2), C gives an idea about the thickness of the boundary layer, values of K_{dif} and C were calculated from the slopes of q_t versus $t^{1/2}$
Elovich Describing the kinetics of heterogeneous chemisorption	$q_t = \frac{1}{\beta}\ln(\alpha\beta) + \frac{1}{\beta}\ln(t)$ α and β are constants of Elovich-type equation α represents the rate of chemisorptions. β is related to the extent of surface coverage and the activation energy of chemisorptions	Plot the values of q_t *Vs* ln (t) to give a linear relationship from which α and β can be determined from the slope and intercept, respectively, q_t is concentration of adsorbate in solid phase at time (t)
Thermodynamic studies	$K_0 = \frac{C_0}{C_e}$ $\Delta G^0 = -RT\ln K_0$	K_0 is equilibrium constant, $\Delta G°$ is change in Gibb's free energy, R is gas constant, T is absolute temperature, $\Delta S°$ is change in entropy, $\Delta H°$ is change enthalpy

mechanism of the reactions (Table 2). An adsorption process is normally controlled by: (1) transport of the solute from solution to the film surrounding the adsorbent, (2) from the film to the adsorbent surface and (3) from the surface to the internal sites followed by binding of analyte to the active sites. The slowest steps out of all the steps determine the overall rate of the adsorption process. If the kinetic model is correct, the appropriate plot of the concentration–time data should be linear (Do 1998). These include pseudo-first-order, pseudo-second-order, parabolic diffusion and Elovich-Type.

The adsorption capability of adsorbent toward nitrate and phosphate can be studied using aqueous solutions of KNO_3 and KH_2PO_4. Adsorption can performed batch-wise in Erlenmeyer flasks on a temperature regulated platform stirrer under the following parameters: temperature 25–55 °C, adsorbent dosage (g/L), pH 2–8, an initial concentration mg/L analyte ions. The pH of the solutions was adjusted by adding either 0.1 M HCl or 0.1 M NaOH. In case, fixed-bed column studies will be performed using a laboratory-scale glass column with an internal diameter of 1 cm and a length of 12 cm. A stainless sieve was attached at the bottom of column with a layer of glass wool. A known quantity of anion solution was fed in upward through the column. The column was operated at three different flow rates ranging 0.5–1.5 mL/min for a solution concentration of 100 mg/L, a bed height of 12 cm, pH = 2–8 and 25 °C. Effluent samples were collected at the outlet of the column at regular time intervals and analyzed for anion concentration. The breakthrough curves were obtained by plotting the ratio (C/C_0) of anion concentration (C) at time (t) to initial concentration (C_0) versus time (t). The adsorption mechanism of the nitrate and phosphate ions onto adsorbents is significantly dependent on the physicochemical properties of N and P ions and their interaction with the adsorbent surface. Properties of nitrate and phosphate such as the solubility, ionic radius, hydration energy and bulk diffusion coefficient are crucial for the selective adsorption of these ions. These are compiled from different sources (Marcus 1997; Nightingale 1959; Richards et al. 2013; Custelcean and Moyer 2007; Kumar et al. 2014). Some of the important characteristics of inorganic anions are briefed in Table 3.

The immobilization of anions onto the adsorbent also relies on the size of the adsorbent pores, which in some cases is similar or smaller than the ionic and/or hydrated dimensions of the anions. This barrier results in selective anionic adsorption and further results in the formation of inner-sphere, outer-sphere complexes and electrostatic or hydrogen bonding of the anion with the adsorbent surface.

Nanoscale materials

Nanomaterials have a large surface area and high chemical reactivity compared to their corresponding bulk analogues and they can be fabricated in a variety of shapes and various lattice planes are present for reactions (Taniguchi et al. 1974). This is the most important and unique aspect about the nanomaterials for their end use in environmental remediation (Pradeep 2012; Ali 2012). These materials either transform contaminates to the harmless products chemically or adsorb/absorb onto the surfaces/cavities and

Table 3 Properties of nitrate and phosphate ions

Parameter	Nitrate	Phosphate
Molecular formula	NO_3^-	PO_4^{3-}
Charge	Monovalent	Trivalent
Molar mass (g/mol)	62.0049	94.97
Solubility in water (Na salts) (g/L)	912.0 (25 °C)	88.0 (25 °C)
Ionic radius (R_{ion}) ($\times 10^{-10}$ m)	3.0	–
Hydrated radius (R_{hyd}) ($\times 10^{-10}$ m)	5.1	3.39
Hydration-free energy (ΔG_{hyd}) (kJ/mol)	− 305.85	–
Bulk diffusion coefficient, 25 °C (D_w) ($\times 10^{-9}$ m^2/s)	1.9	–

hence removing/scavenging them (Bhattacharya et al. 2013; Pradeep 2009). To emphasize recent advances in the development of nanoscale materials for removing nitrate and phosphate ions from water system. We have selected three classes of nanoscale materials that are being evaluated as functional materials for removing these contaminates such as (1) zero-valent metal-containing nanoparticles (ZVMNP), (2) nanoscale metal oxide and metal hydroxides materials (3) functionalized and carbon-based nanomaterials.

Nanoscale zero-valent materials

In comparison with larger-sized zero-valent particles (ZVPs), nZVPs have a greater reactivity due to a greater surface area to volume ratio (Wang and Zhang 1997). The most widely studied ZVNPs for environmental remediation are nanoscale zero-valent iron (nZVI). Synthesis of nZVI particles is quite easy, involving the reduction of ferric ion by sodium borohydride (Wang and Zhang 1997). Typical groundwater contains many dissolved electron acceptors (nitrate or sulfate) that can react with nZVI surface and produce iron surface passivation (Fig. 1).

The nitrate removal can be enhanced by lowering the pH by using either adding acidic solutions or buffer system. However, addition of acidic solution like sulfuric acid (Huang et al. 1998), hydrochloric acid and acetic acid (Cheng et al. 1997) may be effective in lowering the pH, but it also introduces species that has adverse impact on the quality of the drinking water. An alternative procedure to lower the pH is through the use of carbon dioxide bubbling (Ruangchainikom et al. 2006) since it can create an acidic environment by supplying the system with hydrogen ion (Hsu et al. 2011). Effect of both contaminant and solute concentrations on nZVI performance has been investigated in several studies shown in Table 4. Phosphate removal by nZVI and iron oxide nanoparticles is known to be a sorptive process, and the sorbed phosphate remains in the nanoparticles or sometimes get precipitated with iron species (Fig. 1).

Almeelbi and Bezbaruah 2012 have reported up to 100% removal of phosphate using nZVI particles and found these particles to be more efficient than larger-sized particles (micro-ZVI). Effectiveness of the NZVI in phosphate removal was found to 13.9 times higher than micro-ZVI (μZVI) particles with same nZVI and μZVI surface area concentrations used in batch reactors. A phosphate recovery better at higher pH and it decreased with lowering of the pH of the aqueous solution and 20% G-nZVI would remove phosphorus most efficiently. The specific reaction mechanism for the removal of phosphorus with nZVI or G-nZVI was mainly due to chemical reaction between nZVI and phosphorus (Liu et al. 2014). In an another report, ZVI (Wen et al. 2014) was used to remove phosphate from aqueous solution, and the influence of pH, ionic strength and coexisting anions on phosphate removal, results agree well with both Langmuir model and Freundlich model.

Alessio (2015) have reported an efficiency of nitrate removal up to 98% was reached in 60 min during the treatment of solutions with initial nitrate nitrogen concentrations

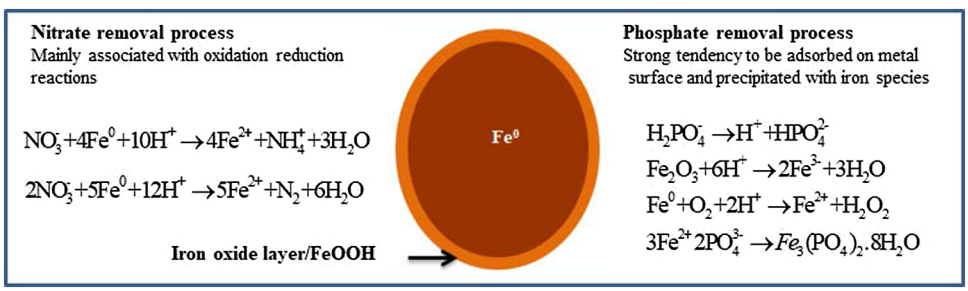

Fig. 1 Possible mechanism of nitrate and phosphate removal using nano zero-valent iron (nZVI) nanoparticles

Table 4 Performance of nano zerovalent particles (nZVP) for the removal of nitrate and phosphate pollutants. ZVI: zero-valent iron

Adsorbent	Amount taken (mg/L)	pH/time (min)	Surface area (m^2/g)	Model and reaction rate	Adsorption capacity (%)	References
nZVI-graphite	100	6.7/30	6.2	–	80/NO_3^-	Zang et al. (2006)
nano-Fe/Cu	100	4/200	33.0	–	60/NO_3^-	Hosseini et al. (2011)
nZVI	100	6–8/5 h	7.7	–	80/NO_3^-	Hsu et al. (2011)
nZVI	100	7/90	93.8	Pseudo-first-order kinetics	97/NO_3^-	Hwang et al. (2011)
nZVI/Fe-Ag/EDTA	1000	4/240	48.1	–	340/NO_3^-	Kunwar et al. (2012)
nZVI	1–10	4/30	–	–	96–100/PO_4^{3-}	Almeelbi and Bezbaruah (2012)
G-nZVI	1–20	– 80	–	Freundlich	15/PO_4^{3-}	Liu et al. (2014)
nZVI	50–90	3–5/60	39.4	First-order	63–98/NO_3^-	Alessio (2015)
Cu–Pd/NZVI	30	7/9 h	–	First-order	–	Hamid et al. (2015)
Nanoscopic Fe^0	50	3/60	39.4	First-order kinetic	98/NO_3^-	Biswas and Bose (2005)
nZVI—graphene	20	– 30	–	Freundlich	16/NO_3^-	Peng et al. (2015)
nZVI	50	11/180	17.6	Langmuir–Hinshelwood pseudo-first-order	50/NO_3^-	Kim et al. (2016)

of 50 mg/L and interaction was verified found to be a first-order kinetic-type. nZVI prepared by chemical reduction without a stabilizing agent and possible mechanism between nitrate ion would be absorbed on the nZVI shell structure, and then the reduction reaction occurred on the shell structure by electron transfer from the core structure (Hwang et al. 2011). Moreover, the reduced ammonium ion would be isolated to the aqueous phase, and it was stripped to the gas phase under an alkaline condition. The nitrate reduction by nZVI is a heterogeneous catalytic reaction and it governs the pseudo-first-order and pseudo-second-order adsorption kinetic equations provided a good fit for the nitrate removal, whereas the Langmuir–Hinshelwood kinetic equation provided a good fit for the ammonia generation (Kim et al. 2016). nZVI particles supported on micro-scale exfoliated graphite were prepared by using KBH_4 as reducing agent in the H_2O/ethanol system (Zang et al. 2006). The supported ZVI materials generally have higher activity and greater flexibility for nitrate removal to the extent of 80% in the near neutral pH range. Bimetallic of nano-Fe/Cu particles was synthesized and used in packed sand column experiments to reduce NO_3^-–N through packed sand column (Hosseini et al. 2011). The rate of reduction by bimetallic particles is significantly faster than those observed for Fe^0 alone (Wang and Chen 1999). The mechanism responsible for this reactivity is related to catalytic hydrogenation and electrochemical effect (Tratnyek et al. 2003). In addition, a higher stability for the degradation and the prevention of the formation and accumulation of toxic by-products are the advantages of bimetallic nanoparticles. Nitrate removal using nZVI supported Cu–Pd bimetallic catalyst (Hamid et al. 2015) in a continuous reactor system. Advantages of their study were found to be higher removal efficiency, relatively mild conditions and easier operation compared to other physico-chemical and biological technologies. A small pilot-scale study was explored for nitrate removal by nZVI particles in a re-circulated flow reactor of 4.3 L liquid volume (Hsu et al. 2011). Nitrate removal of 70% was observed with the initial pH of 6.4 with the solution being pre-purged by N_2 gas at a rate of 50 mL/min. The solution pH needs to be controlled within the neutral range to improve the nitrate removal by the nZVI process. In another report, nitrate-contaminated water passing through reactive porous media comprising of 125 cm^3 of sand containing 0.5, 1.0 or 1.5 g of steel wool and seeded with hydrogenotrophic denitrifying microorganism was sufficient to reduce nitrate concentrations from 40 mg/L as NO_3^-–N to less than 2 mg/L as NO_3^-–N with a retention time of 13 days (Biswas and Bose 2005). A mathematical model was developed to evaluate the performance of nZVI materials role in nitrate reduction, ammonium accumulation and hydrogen turnover (Peng et al. 2015). The simulation results further suggest a nZVI dosing strategy (3–6 mmol/L in temperature range of 30–40 °C, 6–10 mmol/L in temperature range of 15–30 °C and 10–14 mmol/L in temperature range of 5–15 °C) during groundwater remediation to make sure a low ammonium yield and a high nitrogen removal efficiency. EDTA/Fe-Ag nanohybrid material (Kunwar et al. 2012) used for nitrate removal and this interaction verify pseudo-first-order and pseudo-second-order adsorption kinetic equations. In addition, a Langmuir–Hinshelwood

kinetic equation was able to successfully describe ammonia generation, apart from nZVI dose, the ionic strength and effect of pH.

Nanoscale metal oxide and metal hydroxide materials

Metal oxides, metal hydroxides and natural mineral compounds containing these materials are attractive candidates as sorbents for phosphate removal and recovery (Rittmann et al. 2011). These materials exhibit advantages like nontoxic, inexpensive, and chemically stable (Chu et al. 2009; Wong and Lo 2005). The removal efficiency depends on the chemical and physical characteristics (i.e., particle sizes, surface functional groups, specific surface area, metal content and stability) of the sorbents and environmental conditions, such as pH, ion strength, competitive ions, dosage, initial phosphate concentrations and temperature present in solution widely. When low concentrations of phosphate ions occur, bio-treatment and precipitation, methods are not effective. Instead, adsorption methods are recommended as the most effective removal processes for phosphate ions at low concentration. At pH 2–7, H_2PO_4 was dominant species while HPO_4^{2-} became the prime species at pH 8–12. The adsorption-free energy of H_2PO_4 was lower than HPO_4^{2-} so H_2PO_4 was more easily adsorbed onto the surfaces of adsorbents than HPO_4^{2-}. The mechanism of nitrate adsorption by various nanomaterials is based on the electrostatic attraction or ligand-exchange reaction between nitrate and hydroxyl ions depending on the pH of the medium (Golestanifar et al. 2015; Demiral and Gunduzoglu 2010) (Fig. 2).

Hydrated metal oxides like Fe(III), Zr(IV) and Cu(II) have been more extensively explored for phosphate removal (Table 5) because they exhibit a strong ligand sorption (of HPO_4^{2-} and $H_2PO_4^-$) through the formation of inner-sphere complexes or through outer-sphere complexes (Chen et al. 2015). Batch, equilibrium and column experiments were conducted by using Bayoxide E33 and its derivatives to determine various adsorption parameters (Jacob et al. 2016). Equilibrium data were fitted to different adsorption isotherms, and the Langmuir isotherm provided the best fit. Based on the Langmuir model, it was found that E33/Ag II has a slightly higher maximum monolayer adsorption capacity (38.8 mg/g) when compared to unmodified E33 (37.7 mg/g). The uptake of phosphate by zeolite and lanthanum hydroxide (La-ZFA) was explained on the basis of the adsorption mechanism of the ligand-exchange process (Xie et al. 2014). The sorbed phosphate could be recovered by hydrothermal treatment in 3 M NaOH at 250 °C, with a simultaneous regeneration of La-ZFA. The sorbent has a high phosphate removal capacity, with a sorption maximum of 71.94 mg/g, according to the Langmuir model. The removal of phosphate by La-ZFA performs well at a wide pH range, reaching > 95% from pH 2.5 to pH 10.5 when initial P concentration < 100 mg/L. The sorbent Fe–Mg–La with Fe/Mg/La molar ratio of 2:1:1 $Fe(NO_3)_3 9H_2O$, $MgSO_4 H_2O$ and $La(NO_3)_3 6H_2O$ was prepared through co-precipitation approach for phosphate removal in contaminated water (Yang and Chen 2015). The hydroxyl groups play a key role in the phosphate removal by the sorbent and the presence of sulfate groups also play a certain role in the uptake. The spent sorbent can be successfully regenerated by 0.5 M NaOH solution. Yu and Paul Chen (2015) have reported three different magnetic core–shell Fe_3O_4@LDHs composites, Fe_3O_4@Zn–Al–, Fe_3O_4@Mg–Al–, and Fe_3O_4@Ni–Al–LDH were prepared via co-precipitation method for phosphate adsorptive removal. The surface hydroxyl groups (M–OH) may well be exchanged by the adsorbed phosphate, forming outer-sphere surface complex (M–O–P). Therefore, the removal efficiency of phosphate was more than 80% at pH 3–7. A nanostructured Fe–Al–Mn trimetal oxide synthesized by oxidation and co-precipitation method was reported (Lu et al. 2013). The phosphate removal gradually decreased with the increasing of pH (4–10.5). The phosphate

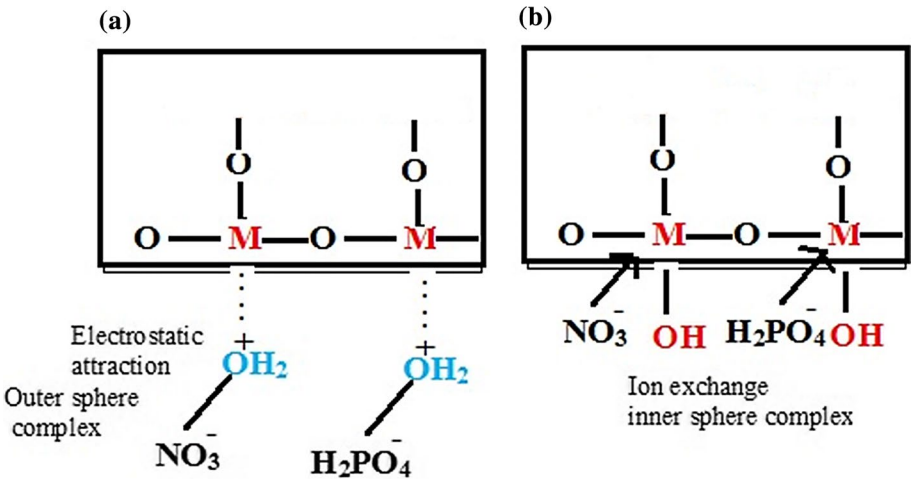

Fig. 2 Possible mechanism of phosphate and nitrate removal using **a** metal oxide and **b** metal hydroxide nanoparticles

Table 5 Performance of nanoscale metal oxide materials for the removal of nitrate and phosphate pollutants

Adsorbent	Amount taken (mg/L)	pH and time (min)	Surface area (m^2/g)	Model and reaction rate	Adsorption capacity (mg/g)	References
Bayoxide-E33	140	7.0 45	120–200	Langmuir model intra-particle diffusion studies	38.8 PO_4^{3-}	Jacob et al. (2016)
Z-$La(OH)_3$	500	2.5–10.524 h	55.69	Langmuir model pseudo-second-order reaction	71.94 PO_4^{3-}	Xie et al. (2014)
Fe–Mg–La	100	6.4 10 h	–	Langmuir model intra-particle diffusion studies	48.3 PO_4^{3-}	Yu and Paul Chen (2015)
Fe–Al–Mn trimetal oxide	4.7−8.7	6.8 200 min	303	Freundlich model pseudo-second-order	48.3 PO_4^{3-}	Lu et al. (2013)
Fe–Ti bimetal oxide	50	6.8 32 h	39.9	Langmuir model pseudo-second-order reaction	35.4 at pH 6.8. PO_4^{3-}	Lu et al. (2015)
n-HZO	10	6.8 6 h	2.34	Langmuir pseudo-first-order	21.1 PO_4^{3-}	Chen et al. (2015)
n-$Mg(OH)_2$	10	6.0–12 80–100	–	Freundlich pseudo-first-order	45.6 PO_4^{3-}	Zhang et al. (2015)
Fe_3O_4/ZrO_2/chitosan	NO_3^- (100) PO_4^{3-} (50)	3 1440	212.9	Langmuir isotherm model	NO_3^- (89) PO_4^{3-} (26.5)	Jiang et al. (2013)
MgO-biochar	–	–	–	–	NO_3^- (94) PO_4^{3-} (835)	Zhang et al. (2012)
Fe–Zr binary oxide	0–35	5.5 6 h	339	Langmuir model pseudo-second-order	PO_4^{3-} (33.4)	Ren et al. (2012)
CuO	200	5.5 180 min	200	Langmuir model pseudo-second-order	PO_4^{3-} (23.9)	Mahdavi and Akhzari (2015)

adsorption on the adsorbent was fitted by Freundlich > Temkin > Langmuir at pH 6.8. The maximum adsorption capacity for Fe–Al–Mn trimetal oxide was about 48.3 mg/g at 25 °C. Spectroscopic analyses indicated that electrostatic attraction and replacement of surface hydroxyl groups (M-OH) by phosphate via the formation of inner-sphere complex were the main adsorption mechanism. The kinetics tests indicated that the phosphate sorption on Fe–Ti bimetal oxide at pH 6.8 obeyed the pseudo-second-order kinetics (Lu et al. 2015). The Langmuir sorption capacity for phosphate was 35.4 mg/g at pH 6.8. Spectroscopic analyses indicated that phosphate sorption on the Fe–Ti bimetal oxide occurred via replacement of surface hydroxyl groups (M-OH) by phosphate. The Fe–Ti bimetal oxide effectively regenerated by NaOH solutions. Nanosized hydrous zirconium oxide (HZO) supported by a macroporous anion exchanger D-201 exhibited highly preferable removal of phosphate from water even in the presence of other commonly occurring anions at greater levels (Chen et al. 2015). Nano-$Mg(OH)_2$ onto macroporous polystyrene beads modified with fixed quaternary ammonium groups [$CH_2N^+(CH_2)_3Cl$] (Zhang et al. 2015). The N^+-tailored groups can accelerate the diffusion of target phosphate through electrostatic attractions. Kinetic equilibrium of phosphate adsorption can be achieved within 100 min, and the calculated maximum adsorption capacity is 45.6 mg/g. The Fe_3O_4/ZrO_2/chitosan composite used to adsorb both nitrate and phosphate (Jiang et al. 2013). Further, this was the first report of a modified chitosan with the ability to adsorb both of these two nutrient anions. The maximum adsorption amount of nitrate and phosphate is 89.3 mg/g and 26.5 mg P/g, respectively. The adsorption process fits well to the pseudo-first-order kinetic rate model, and the mechanism involves simultaneous adsorption and intra-particle diffusion. Zhang et al. (2012) have developed porous MgO-biochar nanocomposites by crystallizing nano-MgO flakes in biochar matrix through slow pyrolysis of $MgCl_2$-pretreated biomass. The Langmuir maximum capacity of phosphate on the MgO-biochar was around 835 mg/g, which is much higher than that of other adsorbents for the removal of phosphate from aqueous solutions. The Langmuir maximum nitrate capacity of MgO-biochar sample was around 94 mg/g. Performance of Fe–Zr binary oxide toward phosphate removal was established by Ren et al. (2012). The adsorption data fitted well to the Langmuir model with the

maximum P adsorption capacity estimated of 24.9 mg P/g at pH 8.5 and 33.4 mg P/g at pH 5.5. The phosphate adsorption was pH dependent, decreasing with an increase in pH value. The presence of chloride, sulfate and carbonate does not interfere on phosphate removal. Mahdavi and Akhzari (2015) reported nanoscale CuO material for the removal of phosphate by adsorption method. Equilibrium adsorption data for phosphate were in good agreement with Langmuir isotherms and pseudo-second-order equation indicating its chemisorption nature adsorption capacity was found to be 23.9 mg/g of CuO. The feasibility of nano-alumina for nitrate ion removal from aqueous solutions was explored by Bhatnagar et al. (2010). The maximum sorption capacity of nano-alumina for NO_3^- removal was found to be 4.0 mg/g. The ligand-exchange reactions between the nitrate ions and surface charge of the adsorbent material took a major role in the NO_3^- adsorption process. Zhang et al. (2012) have reported synthesis of highly porous nanocomposite material consisting of MgO nano-cakes within a biochar matrix for the removal of nitrate from water. The nitrate adsorption capacity for this material was found to be 95 mg/g. The nano-cake structures were regular morphology and dispersed uniformly on the surface of the biochar matrix, making it a potential candidate for nitrate removal from aqueous solution.

Functionalized and carbon-based material

Carbon-based materials like graphite, graphite oxide (GO), graphene, carbon nanotube (CNT), multiwall carbon nanotube (MWCNT) and functionalized carbon-based materials have been made potential applications in sorption. A few studies were reported for the removal of phosphate and nitrate from aqueous phase (Table 6). Kilpimaa et al. (2015) have reported the use of carbon residue obtained from wood gasification for the removal of nitrate and phosphate ions. The kinetics showed that the adsorption data followed pseudo-second-order kinetics and Langmuir model. This may be due to the homogeneous distribution of active sites on physically activated carbon residue. Mahdavi and Akhzari (2015) have used CNT material for the removal of phosphate by adsorption method. Equilibrium adsorption data for phosphate were in good agreement with Freundlich isotherm and pseudo-second-order indicating its chemisorption nature and adsorption capacity was found to be 15.4 mg/g of CNT. ZrO_2 functionalized graphite oxide by post-grafting method and employed it as a sorbent material for the removal of phosphate (Zong et al. 2013). In another report, adsorption capacity of phosphate on ZrO_2 functionalized graphite oxide was found to be highly dependent on the pH values and decreases on increasing the pH value from 2 to 12 and attained its maximum at a pH value of 2. This reduction in the adsorption capacity on increasing pH was explained on the basis of variation in the extent of various types of interaction between phosphate ions and ZrO_2/graphene composite including electrostatic interaction, ion-exchange and acid base interaction. Phosphate removal based on graphene aerogel decorated with goethite (FeOOH) and magnetite (Fe_3O_4) nanoparticles (Diana et al. 2015). The aerogel showed a superior capacity to remove up to

Table 6 Performance of nanoscale carbon-based materials for the removal of nitrate and phosphate pollutants

Adsorbent	Amount taken (mg/L)	pH and time (min)	Surface area (m^2/g)	Model and reaction rate	Adsorption capacity (mg/g)	References
Carbon residue	10	4 (NO_3^-) 6 (PO_4^{3-}) 5 h	590	Langmuir model and pseudo-second-order	30.2 NO_3^- 11.2 PO_4^{3-}	Kilpimaa et al. (2015)
CNT	200	5.6 180 min	12.1	Freundlich isotherms pseudo-second-order kinetic	15.4 PO_4^{3-}	Mahdavi and Akhzari (2015)
GO/ZrO_2	20	6.0 48 h	160	Langmuir adsorption isotherms	16.45 PO_4^{3-}	Zong et al. (2013)
Graphene-FeOOH–Fe_2O_3	200	6 3 h	–	Freundlich model second-order equation	350 PO_4^{3-}	Diana et al. (2015)
Graphene	100	7	–	Langmuir second-order adsorption	89.37 PO_4^{3-}	Vasudevan and Lakshmi (2012)
MCM-48 silica	300	< 8 NO_3^- 4–6 PO_4^{3-} 10	750	Freundlich model	NO_3^- (71%) PO_4^{3-} (88%)	Saad et al. (2007)
Zr(IV)-chitosan	NO_3^- (10) PO_4^{3-} (1000)	3–10 60	9.04	Langmuir and Freundlich	NO_3^-(128) PO_4^{3-} (149)	Sowmya and Meenakshi (2014)

350 mg/g at an initial phosphate concentration of 200 mg/L from aqueous system.

Graphene is an excellent phosphate adsorbent with an adsorption capacity of up to 89.37 mg/g at an initial phosphate concentration of 100 mg/L and temperature of 303 K (Vasudevan and Lakshmi 2012). The adsorption process follows second-order kinetics, suggesting that the adsorption was a chemical controlling process. The adsorption of phosphate preferably fitting the Langmuir adsorption isotherm suggests monolayer coverage of adsorbed molecules. Afkhami et al. (2007) described an effect of functional groups on the adsorption of $NO_3^-$and NO_2^- by carbon cloth. The carbon cloths were chemically etched in 4 M H_2SO_4 solution after deionization cleaning procedure and used for the adsorption of NO_3^- and NO_2^- from water samples at nearly neutral (pH 7) solution. The treatment of carbon cloth with acid produced positive sites on the carbon cloth, by protonation of surface—OH groups caused an increase in electrostatic adsorption of anions, due to this force attraction will be more. The adsorption capacity of acid-treated carbon cloth for NO_3^- and NO_2^- was 2.03 and 1.01 mmol/g, respectively. Powdered activated carbon (PAC) and carbon nanotubes (CNTs) were used for the removal of NO_3^- from aqueous solution (Namasivayam and Sangeetha 2005). The NO_3^- adsorption capacity of CNTs was found to be higher than PAC and decreased above pH 5. The equilibration time for maximum NO_3^- uptake was 60 min. Adsorption capacity of the PAC and CNTs was found to be 10 and 25 mmol NO_3^- per gram adsorbent, respectively.

The ordered mesoporous materials' (OMM) with pore size between 2 and 50 nm were discovered in 1992 by researchers working for the Mobil corporation. In 1998, researchers at the University of California in Santa Barbara announced that they had produced silica with much larger 46–300 angstrom pores (Zhao et al. 1998) and latter the material was named Santa Barbara Amorphous type material (SBA-15). Surface-modified mesoporous silica materials produced by surface functionalization via the tethering of organic functional groups are potential adsorbents used for removal of water pollutants. Saad et al. (2007) have reported 46 and 43 mg/g adsorption capacity when using ammonium functionalized MCM-48 for phosphate and nitrate ions removal, respectively. In another report (Saad et al. 2008), synthesized and protonated several amino-functionalized mesoporous silica materials and successfully applied them to remove nitrate from water. The aminated and protonated mesoporous silica showed high adsorption capacities of 0.6–2.4 mg/g for the unmodified mesoporous silica, despite the latter having a high surface area total pore volume. Phosphate was found to reduce nitrate adsorption; therefore, special types of functionalized mesoporous silicas (SBA-15) were produced where the nitrate adsorption was less affected by phosphate due to pore size of adsorbent matching with nitrate ion. Unmodified cross-linked chitosan beads do not have the ability to remove nitrate and phosphate due to the absence of positive sites. Zr(IV) was loaded onto cross-linked chitosan beads to make the polymer selective toward the nitrate and phosphate anions (Sowmya and Meenakshi 2014). Zirconium-based adsorbents have excellent anion adsorption capacities. Zr(IV)-loaded sugar beet pulp was used for the removal of nitrate (Hassan et al. 2010), mesoporous ZrO_2 (Liu et al. 2014), amorphous zirconium hydroxide (Chitrakar et al. 2006) and Zr^{4+} introduced Mg–Al LDH (Chitrakar et al. 2007) were the various zirconium-based materials reported for the removal of phosphate.

Conclusions

A critical evaluation of nanoscale materials as sorbents for the removal of nitrate and phosphate from aqueous phase has been made in this manuscript. These materials are capable to remove pollutants even at low concentration, under varied conditions of pH and temperature. The dose required of nanoparticles is quite low, making their application very economical. Moreover, it has been observed that the removal time is quite fast. These properties of nanoparticles made them ideal candidates for fast and inexpensive water treatment technology.

Acknowledgements Authors are thankful to the administration of VIT University, Vellore, India, for providing infrastructures to write this article and carry out other research.

References

Afkhami A, Madrakian T, Karimi Z (2007) The effect of acid treatment of carbon cloth on the adsorption of nitrite and nitrate ions. J Hazard Mater 144:427–431. https://doi.org/10.1016/j.jhazmat.2006.10.062

Alessio S (2015) Use of nanoscale zero-valent iron (NZVI) particles for chemical denitrification under different operating conditions. Metals 5:1507–1519. https://doi.org/10.3390/met5031507

Ali I (2012) New generation adsorbents for water treatment. Chem Rev 112:5073–5091. https://doi.org/10.1021/cr300133d

Almeelbi T, Bezbaruah A (2012) Aqueous phosphate removal using nanoscale zero-valent iron. J Nanopart Res 14:1–14. https://doi.org/10.1007/s11051-012-0900-y

APHA (1985) Standard methods for examination of water and wastewater, 20th edn. American Public Health Association, Washington, DC

APHA (1998) Standard methods for examination of water and wastewater, 20th edn. American Public Health Association, Washington, DC

Bhatnagar A, Kumar E, Sillanpaa M (2010) Nitrate removal from water by nano-alumina: characterization and sorption studies. Chem Eng J 163:317–323. https://doi.org/10.1016/j.cej.2010.08.008

Bhattacharya S, Saha I, Mukhopadhyay A et al (2013) Role of nanotechnology in water treatment and purification: potential applications and implications. Int J Chem Sci Technol 3:59–64

Biswas S, Bose P (2005) Zero-valent iron-assisted autotrophic denitrification. J Environ Eng 131:1212–1220. https://doi.org/10.1061/(ASCE)0733-9372(2005)131:8(1212)

Chen L, Zhao X, Pan B et al (2015) Preferable removal of phosphate from water using hydrous zirconium oxide-based nanocomposite of high stability. J Hazard Mater 284:35–42. https://doi.org/10.1016/j.jhazmat.2014.10.048

Cheng IF, Muftikian R, Fernando Q, Korte N (1997) Reduction of nitrate to ammonia by zero-valent iron. Chemosphere 35:2689–2695. https://doi.org/10.1016/S0045-6535(97)00275-0

Chitrakar R, Tezuka S, Sonoda A et al (2006) Selective adsorption of phosphate from seawater and wastewater by amorphous zirconium hydroxide. J Colloids Interface Sci 297:426–433. https://doi.org/10.1016/j.jcis.2005.11.011

Chitrakar R, Tezuka S, Sonoda A et al (2007) Synthesis and phosphate uptake behavior of Zr^{4+} incorporated MgAl-layered double hydroxides. J Colloids Interface Sci 313:53–63. https://doi.org/10.1016/j.jcis.2007.04.004

Chu L, Yan S, Xing XH, Sun X, Jurcik B (2009) Progress and perspectives of sludge ozonation as a powerful pretreatment method for minimization of excess sludge production. Water Res 43(7):1811–1822. https://doi.org/10.1016/j.watres.2009.02.012

Custelcean R, Moyer B (2007) Anion separation with metal-organic frameworks. Eur J Inorg Chem. https://doi.org/10.1002/ejic.200700018

Demiral H, Gunduzoglu G (2010) Removal of nitrate from aqueous solutions by activated carbon prepared from sugar beet bagasse. Bioresour Technol 101:1675–1680. https://doi.org/10.1016/j.biortech.2009.09.087

Diana NH, Shervin K, Luoshan W, Dusan L (2015) Engineered graphene—nanoparticle aerogel composites for efficient removal of phosphate from water. J Mater Chem A 3:6844–6852. https://doi.org/10.1039/c4ta06308b

Do DD (1998) Adsorption analysis: equilibria and kinetics. Imperial College Press, London

EPA (1990) Estimated national occurrence and exposure to nitrate/nitrite in public drinking water supplies. U.S. Environmental Protection Agency, Washington, pp 2–32

EPA (2000) Wastewater technology fact sheet chemical precipitation. US Environmental Protection Agency, Washington

Eugene WR et al (1985) Standard methods for examination of water and wastewater, 20th edn. American public health association, Washington

Eugene WR et al (1998) Standard methods for examination of water and wastewater, 20th edn. American Public Health Association, Washington

Golestanifar H, Asadi A, Alinezhad A, Haybati B, Vosoughi M (2015) Isotherm and kinetic studies on the adsorption of nitrate onto nanoalumina and iron-modified pumic. Desalin Water Treat. https://doi.org/10.1080/19443994.2014.1003975

Hamid S, Bae S, Lee W, Amin MT, Alazba AA (2015) Catalytic nitrate removal in continuous bimetallic Cu–Pd/nanoscale zerovalent iron system. Ind Eng Chem Res 54(24):6247–6257. https://doi.org/10.1021/acs.iecr.5b01127

Hassan ML, Kassem NF, Abd El-Kader AH (2010) Novel Zr(IV)/sugar beet pulp composite for removal of sulfate and nitrate anions. J Appl Polymer Sci 117(4):2205–2212. https://doi.org/10.1002/app.32063

Hell F, Lahnsteiner J, Frischherz H, Baumgartner G (1998) Experience with full-scale electrodialysis for nitrate and hardness removal. Desalination 117:173–180. https://doi.org/10.1016/S0011-9164(98)00088-5

Hosseini SM, Ataie-Ashtiani B, Kholghi M (2011) Nitrate reduction by nano-Fe/Cu particles in packed column. Desalination 276:214–221. https://doi.org/10.1016/j.desal.2011.03.051

Hsu J, Liao C, Wei Y (2011) Nitrate removal by synthetic nanoscale zero-valent iron in aqueous recirculated reactor. Sustain Environ Res 21(6):353–359

Huang CP, Wang HW, Chiu PC (1998) Nitrate reduction by metallic iron. Water Res 32:2257–2264. https://doi.org/10.1016/S0043-1354(97)00464-8

Hwang YH, Kim DG, Shin HS (2011) Mechanism study of nitrate reduction by nano zero valent iron. J Hazard Mater 185:1513–1521. https://doi.org/10.1016/j.jhazmat.2010.10.078

Jacob L, Han C, Li X, Dionysiou DD, Nadagouda MN (2016) Phosphate adsorption using modified iron oxide-based sorbents in lake water: kinetics, equilibrium, and column test. Chem Eng J 284:1386–1396

Jiang JQ, Graham NJD (1998) Pre-polymerised inorganic coagulants and phosphorus removal by coagulation—a review. Water SA 24:237–244

Jiang H, Chen P, Luo S et al (2013) Synthesis of novel nanocomposite Fe_3O_4/ZrO_2/chitosan and its application for removal of nitrate and phosphate. Appl Surf Sci 284:942–949. https://doi.org/10.1016/j.apsusc.2013.04.013

Kilpimaa S, Runtti H, Kangas T et al (2015) Physical activation of carbon residue from biomass gasification: novel sorbent for the removal of phosphates and nitrates from aqueous solution. J Ind Eng Chem 21:1354–1364. https://doi.org/10.1016/j.jiec.2014.06.006

Kim DG, Hwang YH, Shin HS, Ko SO (2016) Kinetics of nitrate adsorption and reduction by nano-scale zero valent iron (NZVI): effect of ionic strength and initial pH. KSCE J Civ Eng 20(1):175–187. https://doi.org/10.1007/s12205-015-0464-3

Kraemer EO (1930) Treatise on physical chemical chemistry. In: Taylor HS (ed.), II edn Vol II, D. Van Nostrand Co., Inc., New York, p 74

Kumar E, Bhatnagar A, Hogland W et al (2014) Interaction of anionic pollutants with Al-based adsorbents in aqueous media—a review. Chem Eng J 241:443–456. https://doi.org/10.1016/j.cej.2013.10.065

Kunwar PS, Arun KS, Shikha G (2012) Zero-valent bimetallic nanoparticles in aqueous medium. Environ Sci Pollut Res 19(9):3914–3924. https://doi.org/10.1007/s11356-012-1005-y

Liu F, Yang J, Zuo J et al (2014) Graphene-supported nanoscale zero-valent iron: removal of phosphorus from aqueous solution and mechanistic study. J Environ Sci 26:1751–1762. https://doi.org/10.1016/j.jes.2014.06.016

Lu J, Liu H, Liu R et al (2013) Adsorptive removal of phosphate by a nanostructured Fe–Al–Mn trimetal oxide adsorbent. Powder Technol 233:146–154. https://doi.org/10.1016/j.powtec.2012.08.024

Lu J, Liu D, Hao J et al (2015) Phosphate removal from aqueous solutions by a nano-structured Fe–Ti bimetal oxide sorbent. Chem Eng Res Des 93:652–661. https://doi.org/10.1016/j.cherd.2014.05.001

Mahdavi S, Akhzari D (2015) The removal of phosphate from aqueous solutions using two nano-structures: copper oxide and carbon tubes. Clean Technol Environ Policy. https://doi.org/10.1007/s10098-015-1058-y

Marcus Y (1997) Ion properties. CRC Press, Dekker, New York

Namasivayam C, Sangeetha D (2005) Removal and recovery of nitrate from water by $ZnCl_2$ activated carbon from coconut coir pith, an agricultural solid waste. Indian J Chem Technol 12:513–521. https://doi.org/10.1016/j.chemosphere.2005.02.051

Nightingale R (1959) Phenomenological theory of ion solvation. Effective radii of hydrated ions. J Phys Chem 63:1381–1387. https://doi.org/10.1021/j150579a011

Peng L, Liu Y, Gao SH et al (2015) Evaluation on the nanoscale zero valent iron based microbial denitrification for nitrate removal from groundwater. Sci Rep 5:12331. https://doi.org/10.1038/srep12331

Pradeep T (2009) Noble metal nanoparticles for water purification: a critical review. Thin Solid Films 517:6441–6478. https://doi.org/10.1016/j.tsf.2009.03.195

Pradeep T (2012) A text book of nanosceince and nanotechnology. Tata McGraw Hill Education Pvt Ltd, New Delhi

Prashantha Kumar TKM, Sangeetha P, Revathi SK, Ashok Kumar SK (2016) Selective removal of nitrate and phosphate from wastewater using nanoscale materials. Sustain Agric Rev 3:13. https://doi.org/10.1007/978-3-319-48009-1_8

Rademacher JJ, Young TB, Kanarek MS (1992) Gastric cancer mortality and nitrate levels in Wisconsin drinking water. Arch Environ Heal 47:292–294. https://doi.org/10.1080/00039896.1992.9938364

Razzaque MS (2011) Phosphate toxicity: new insights into an old problem. Clin Sci (Lond) 120(3):91–97. https://doi.org/10.1042/CS20100377

Ren Z, Shao L, Zhang G (2012) Adsorption of phosphate from aqueous solution using an iron–zirconium binary oxide sorbent. Water Air Soil Pollut 223:4221–4231. https://doi.org/10.1007/s11270-012-1186-5

Richards L, Richards BS, Corry B, Schafer AI (2013) Experimental energy barriers to anions transporting through nanofiltration membranes. Environ Sci Technol 47:1968–1976. https://doi.org/10.1021/es303925r

Rittmann BE, Mayer B, Westerhoff P, Edwards M (2011) Capturing the lost phosphorus. Chemosphere 84(6):846–853. https://doi.org/10.1016/j.chemosphere.2011.02.001

Ruangchainikom C, Liao CH, Anotai J, Lee MT (2006) Characteristics of nitrate reduction by zero-valent iron powder in the recirculated and CO_2 bubbled system. Water Res 40:195–204. https://doi.org/10.1016/j.watres.2005.09.047

Saad R, Belkacemi K, Hamoudi S (2007) Adsorption of phosphate and nitrate anions on ammonium-functionalized MCM-48: effects of experimental conditions. J Colloids Interface Sci 311:375–381. https://doi.org/10.1016/j.jcis.2007.03.025

Saad R, Hamoudi S, Belkacemi K (2008) Adsorption of phosphate and nitrate anions on ammonium-functionalized mesoporous silicas. J Porous Mater 15:315–323. https://doi.org/10.1007/s10934-006-9095-x

Schumann U, Huntrieser H (2007) The global lightning-induced nitrogen oxides source. Atmos Chem Phys Discuss 7:2623–2818. https://doi.org/10.5194/acpd-7-2623-2007

Sowmya A, Meenakshi S (2014) Zr(IV) loaded cross-linked chitosan beads with enhanced surface area for the removal of nitrate and phosphate. Int J Biol Macromol 69:336–343. https://doi.org/10.1016/j.ijbiomac.2014.05.043

Tan IW, Ahmad L, Hameed BH (2008) Optimization of preparation conditions for activated carbons from coconut husk using response surface methodology. Chem Eng J 137:462–470. https://doi.org/10.1016/j.cej.2007.04.031

Taniguchi N, et al (1974) On the basic concept of nanotechnology. In: Proceedings of the international conference on production engineering, Tokyo, Part II, Japan Society of Precision Engineering, pp 18–23

Theodore L, Ricci F (2010) Mass transfer operations for the practicing engineer. Wiley, Hoboken

Tratnyek PG, Scherer MM et al (2003) Permeable reactive barriers of iron and other zero-valent metals. In: Tarr MA (ed) Chemical degradation methods for wastes and pollutants: environmental and industrial applications. Marcel Dekker, New York, pp 371–421

Vasudevan S, Lakshmi J (2012) The adsorption of phosphate by graphene from aqueous solution. RSC Adv 2:5234. https://doi.org/10.1039/c2ra20270k

Wang CY, Chen ZY (1999) The preparation, surface modification, and characterization of metallic nanoparticles. Chin J Chem Phys 12:670–674

Wang CB, Zhang WX (1997) Synthesizing nanoscale iron particles for rapid and complete dechlorination of TCE and PCBs. Environ Sci Technol 31:2154–2156. https://doi.org/10.1021/es970039c

Wen Z, Zhang Y, Dai C (2014) Removal of phosphate from aqueous solution using nanoscale zerovalent iron (nZVI). Colloids Surf A Physicochem Eng Asp 457:433–440. https://doi.org/10.1016/j.colsurfa.2014.06.017

WHO: World Health Organization (2011) Guidelines for drinking water Quality, 4th edn. http://www.apps.who.int/iris/bitstream/10665/44584/1/9789241548151_eng.pdf

Wong WT, Lo KV (2005) Release of phosphorus from sewage sludge using microwave technology. J Environ Eng Sci 4(1):77–81. https://doi.org/10.1139/s04-056

Xie J, Wang Z, Fang D et al (2014) Green synthesis of a novel hybrid sorbent of zeolite/lanthanum hydroxide and its application in the removal and recovery of phosphate from water. J Colloids Interface Sci 423:13–19. https://doi.org/10.1016/j.jcis.2014.02.020

Yang Y, Chen JP (2015) Key factors for optimum performance in phosphate removal from contaminated water by a Fe–Mg–La tri-metal composite sorbent. J Colloids Interface Sci 445:303–311

Yu Y, Paul Chen J (2015) Key factors for optimum performance in phosphate removal from contaminated water by a Fe–Mg–La tri-metal composite sorbent. J Colloids Interface Sci 445:303–311. https://doi.org/10.1016/j.jcis.2014.12.056

Zang H, Jin ZH, Han CH (2006) Synthesis of nanoscale zero-valent iron supported on exfoliated graphite for removal of nitrate. Trans Nonferrous Met Soc China 16:345–349

Zhang M, Gao B, Yao Y et al (2012) Synthesis of porous MgO-biochar nanocomposites for removal of phosphate and nitrate from aqueous solutions. Chem Eng J 210:26–32. https://doi.org/10.1016/j.cej.2012.08.052

Zhang Q, Zhang Z, Teng J, Huang H (2015) Highly efficient phosphate sequestration in aqueous solutions using nano-magnesium hydroxide modified polystyrene materials. Ind Eng Chem Res 54:2940–2949. https://doi.org/10.1021/ie503943z

Zhao D, Huo Q, Feng J et al (1998) Nonionic triblock and star diblock copolymer and oligomeric sufactant syntheses of highly ordered, hydrothermally stable, mesoporous silica structures. J Am Chem Soc 120:6024–6036. https://doi.org/10.1021/ja974025i

Zong E, Wei D, Wan H et al (2013) Adsorptive removal of phosphate ions from aqueous solution using zirconia-functionalized graphite oxide. Chem Eng J 221:193–203. https://doi.org/10.1016/j.cej.2013.01.088